



Control of Visually Guided Behavior by Distinct Populations of Spinal Projection Neurons

Citation

Orger, Michael B., Adam R. Kampff, Kristen E. Severi, Johann H. Bollmann, and Florian Engert. 2008. Control of visually guided behavior by distinct populations of spinal projection neurons. *Nature Neuroscience* 11(3): 327-333.

Published Version

doi:10.1038/nn2048

Permanent link

<http://nrs.harvard.edu/urn-3:HUL.InstRepos:11204671>

Terms of Use

This article was downloaded from Harvard University's DASH repository, and is made available under the terms and conditions applicable to Open Access Policy Articles, as set forth at <http://nrs.harvard.edu/urn-3:HUL.InstRepos:dash.current.terms-of-use#OAP>

Share Your Story

The Harvard community has made this article openly available.
Please share how this access benefits you. [Submit a story](#).

[Accessibility](#)

Published in final edited form as:

Nat Neurosci. 2008 March ; 11(3): 327–333. doi:10.1038/nn2048.

Control of visually guided behavior by distinct populations of spinal projection neurons

Michael B Orger^{1,3}, Adam R Kampff^{1,3}, Kristen E Severi², Johann H Bollmann¹, and Florian Engert¹

¹Department of Molecular and Cellular Biology, Harvard University, 16 Divinity Avenue, Cambridge, Massachusetts 02138, USA

²Department of Biology, Northeastern University, 360 Huntington Avenue, Boston, Massachusetts 02115, USA

Abstract

A basic question in the field of motor control is how different actions are represented by activity in spinal projection neurons. We used a new behavioral assay to identify visual stimuli that specifically drive basic motor patterns in zebrafish. These stimuli evoked consistent patterns of neural activity in the neurons projecting to the spinal cord, which we could map throughout the entire population using *in vivo* two-photon calcium imaging. We found that stimuli that drive distinct behaviors activated distinct subsets of projection neurons, consisting, in some cases, of just a few cells. This stands in contrast to the distributed activation seen for more complex behaviors. Furthermore, targeted cell by cell ablations of the neurons associated with evoked turns abolished the corresponding behavioral response. This description of the functional organization of the zebrafish motor system provides a framework for identifying the complete circuit underlying a vertebrate behavior.

In a behaving animal, the brain communicates its intentions to muscles via the pattern of activity in descending projection neurons¹. In vertebrates, these cells respond to the detection and processing of sensory stimuli and transmit their motor command to the local networks of the spinal cord, which in turn initiate and coordinate muscle contraction². A fundamental question in neuroscience is how the commands that initiate behaviors are encoded in the activation of these projection neurons^{3–5}.

The spinal projection system of fish provides an excellent model for studying this code⁶. A diverse range of swimming behaviors can be seen in 6-d-old zebrafish^{7–9} that are mediated by a descending projection to the spinal cord consisting of fewer than 300 neurons^{10,11}. These neurons are easily labeled with fluorescent indicators¹², optically accessible with modern imaging techniques and arranged in a stereotyped pattern such that the same cells or groups of cells can easily be identified from one fish to the next¹³. These neurons are morphologically diverse, with distinct dendritic fields and axonal projection patterns^{13,14}, suggesting that they serve different behavioral functions. Nevertheless, determining how differing patterns of activity in these spinal projection neurons produce different motor outputs has proved to be difficult.

© 2008 Nature Publishing Group

Correspondence should be addressed to M.B.O. (morger@mcb.harvard.edu).

³These authors contributed equally to this work.

Note: Supplementary information is available on the Nature Neuroscience website.

An important step toward achieving this goal is to find ways to reliably and specifically activate distinct types of movement. One approach has been to use tactile stimuli to the head and tail of the zebrafish, which evoke different escape swims and differentially activate the segmental homologs of the Mauthner cell¹². Activity in the Mauthner cell is sufficient to initiate escape sequences in goldfish¹⁵. Ablation of these neurons in zebrafish can eliminate short-latency, high-performance turns in response to tactile and acoustic stimuli, but the fish still show slower, long-latency responses^{16,17}, and tactile stimuli have been found to activate virtually all reticulospinal neurons¹⁸. Similar widespread activation of motor-control neurons has been observed in both invertebrate^{19,20} and vertebrate model systems^{21,22}. This suggests that, although small numbers of neurons may be sufficient to activate different behaviors^{23,24}, the actual command is encoded in distributed activity throughout the population of control neurons².

The swimming behaviors of zebrafish, including the complex sequence of turns and swims that make up the escape response, can be broken down into basic kinematic elements⁸. It is possible that the motor commands for these basic behaviors originate from distinct populations of neurons, which when combined would appear as a 'distributed command'. We found that whole-field visual motion, with the direction dynamically locked to the fish's body axis, is able to selectively evoke some of these basic swim patterns. Calcium imaging of stimulus-evoked responses in the complete population of neurons projecting to the spinal cord revealed that these control neurons are indeed organized into distinct functional groups. We established a causal link between this observed organization and control of the fishes' behavior by targeted single-cell ablations.

RESULTS

Behavioral responses to stabilized whole-field motion

Larval zebrafish show a reliable optomotor response, turning and swimming to follow large moving gratings presented from below²⁵. This requires that the fish respond to different stimulus directions with different swimming trajectories. To analyze the components of this complex behavior, we needed to eliminate the effect of the fishes' swimming on the stimulus orientation and motion. We achieved this by tracking the fishes' position and heading using a high-speed camera and translating and rotating the stimulus to cancel the fishes' own motion (Fig. 1a). Thus, if a fish viewing a right-to-left grating turned to the left, the stimulus rotated with him so that he continued to see leftward motion.

We found that the fishes' swimming behavior was strongly tuned for stimulus direction (Fig. 1b). Stabilized gratings moving in 24 different directions relative to the fishes' body axis triggered 24 different swimming trajectories. Gratings moving from tail to head caused vigorous forward swimming; gratings that drift toward the fishes' left or right caused turning in the corresponding direction. The basic swim parameters, forward velocity and angular velocity, both showed strong tuning for stimulus direction (Fig. 1c,d).

Motor patterns underlying the optomotor response

Larval zebrafish swimming behavior occurs in discrete bouts alternating with brief periods of inactivity. These swimming bouts can be grouped into a small number of distinct categories, which have been characterized in detail^{8,9,26}. We analyzed the visually evoked responses at the level of single swim bouts. We compared the high-speed kinematics of three typical swims evoked by different grating directions, a left turn, a right turn and a forward swim (Fig. 1e). The left and right turns consist of a sharp tail flick in one direction in which the tip of the tail bends around up to 180 degrees. This most closely resembles the

previously described spontaneous routine turn⁸. The forward swim consists of ~30-Hz tail oscillations and corresponds to the 'slow swim'⁸.

We compared the distribution of swimming bouts, characterized by two parameters, distance swum forward and angle turned, in response to moving gratings in eight different directions (Fig. 1f). In the center we have superimposed, for comparison, the distributions for forward (tail to head), back left and back right motion. We also plotted the same data using an additional parameter, left-to-right movement (Supplementary Fig. 1 online). Two features of the distributions were clear. First, the responses to each direction were highly clustered, indicating that they are stereotyped across trials and across fish. We observed that 84% of all swim bouts recorded during forward motion propelled the fish forward 0.5–4.0 mm with less than 9° of change in body angle. In contrast, 80% of bouts during back left motion were left turns larger than 45°. Second, there was less than 3% overlap between the distribution of swimming bouts evoked by forward motion and the turning responses shown superimposed in the center panel. From this, we conclude that whole-field drifting gratings can be used to isolate distinct components of zebrafish swimming behavior. Clustering of turns and forward swims was clearly seen when responses to all eight directions were combined (Supplementary Fig. 2 online). The stimulus tuning for each distinct behavior (Fig. 1g) was then compared with the stimulus tuning of neural responses. A complete mapping of neural activity required that the responses persist over multiple presentations of the stimuli. This was the case for the whole-field motion responses, which showed little or no reduction over time (Fig. 1h).

Calcium imaging of responses in spinal projection neurons

All motor commands from the fish's brain to its spinal cord must pass through the array of descending projection neurons. We used calcium imaging to monitor the activation of all such neurons during presentation of the behaviorally relevant stimuli described above. Two-photon excitation was essential, in part because the infrared excitation light was invisible to the fish, but also because it provides access to the deepest cells of the reticulospinal system. Responses were typically stable for several hours, allowing imaging at many focal planes and subsequent reconstruction of the response properties for the whole population.

We illustrate the analysis of such an experiment for a group of cells in the right rhombomere 1 (Fig. 2a). Two example cells are indicated and their calcium responses, averaged over their three-dimensional volume, are plotted (Fig. 2b). The stimulus was a sinusoidal grating that drifted at 1 Hz for 10 s in one of eight directions (shaded regions) and was stationary for 17 s in between. The responses of these two cells were clearly selective for different directions. Notably, all the projection neurons with stimulus-evoked responses ($>0.1 \Delta f/f$ to at least one direction) had strong direction selectivity (Supplementary Fig. 3 online). We plotted the cells' responses, in polar form, as the average percentage increase in fluorescence for each stimulus direction and also as a 'directionality vector'²⁷ (Fig. 2c). We summarized the results of this analysis in a color-coded image (Fig. 2d).

The end result of such an analysis for one fish with scattered labeling throughout the spinal projection system is shown in Figure 2e. Most cells either did not respond or preferred forward motion. A few cells preferred gratings moving in directions that elicited turning. The organization of forward motion-responsive cells seen in this fish was repeated in all of the individuals that we examined. We divided the cells into 20 morphological groups for analysis (a schematic of our classification system is shown in Fig. 2f).

Projection neuron responses to whole-field motion

Identifying the neural correlates of the zebrafish whole-field motion response required a complete mapping of the activity of projection neurons in response to drifting gratings. We analyzed responses from 1,465 neurons in 50 fish (Fig. 3). The cells fell into distinct functional groups. The stimulus tuning of each group could be compared with the stimulus tuning of the behavioral patterns (Fig. 1g), allowing us to hypothesize which of these neurons might participate in each behavior.

Cells involved in initiating slow swims should be selectively activated by forward motion and show bilaterally symmetric responses. Both of these properties were seen for cells in the nucleus of the medial longitudinal fasciculus (nucMLF), including the large MeL and MeM cells, RoL1, RoR1 and RoM1c. In every fish, forward-preferring neurons were scattered throughout the nucMLF (three examples of well-labeled nucMLF cells are shown in Fig. 4a). Cells of the MiR and MiM types also occasionally showed weak forward responses, but this was not consistent across fish.

We expected neurons involved in turning to show two characteristics. They should be activated by stimuli that evoke turns (Fig. 1g), and their responses should be lateralized; a left-preferring neuron should have a contralateral partner with the opposite preference. In only two places were these conditions met: in RoM1r and in the ventromedial cells of rhombomeres 3–5 (red/green/blue box). Cells in the RoM1r group were small and not always well labeled. However, they were clearly identifiable by shape and location and showed notable lateralized response properties selective for 'turn' stimuli. The spatial organization of this direction preference in rhombomere 1 was consistent from fish to fish (Fig. 4b).

The average tuning curve of the ventromedial cells included both bilateral forward-motion responses and lateralized responses to left and right stimuli. However, the response vectors of these cells spanned a wide range of directions. This implies that these cells, although grouped together on the basis of anatomical features, are, in fact, functionally heterogeneous. This was best demonstrated by looking at all ventromedial cells individually in a single fish (Fig. 4c). These clusters contained mixtures of neurons with different response properties. Many cells showed a strong forward-motion preference, but some showed a lateralized preference for turning stimuli. Therefore, this group could be involved in generating both slow swims and turns. We plotted the distribution of preferred directions for neurons in responsive groups (Supplementary Fig. 3), illustrating the bimodal distribution of preferred directions in the ventromedial group. The remaining groups of cells showed no consistent responses, although most of these have been shown to have calcium responses to tactile stimuli¹⁸ and are likely to participate in other behaviors.

Laser ablation of turning neurons

Calcium imaging revealed that projection neurons were organized into distinct functional groups related to distinct behaviors, which suggests that removing one of these groups should result in a loss of its associated behavioral response. To test for the expected causal relationship, we chose to remove neurons responsive to 'turn' stimuli, RoM1r and ventromedial cells, as there are relatively few and the two laterally symmetrical populations provide an internal control. To remove the selected cells, we adapted a technique²⁸ based on nonlinear absorption for the rapid ablation of single identified neurons in the zebrafish. A mode-locked laser is scanned in a spiral pattern over a selected cell until a highly localized plasma is formed²⁹, destroying the target but leaving adjacent cells intact (Fig. 5a–c). To test the efficacy of this technique, we ablated the Mauthner cell and its segmental homologs,

reproducing the side-specific increase in escape response latency that was found in previous studies¹⁶ (**Supplementary Movie 1** online).

We measured the behavioral responses of fish, before and after ablation, to stimuli that reliably evoked turning, backward left and backward right motion. To test the behavior around the threshold for responding, we ramped up the contrast of the stimuli from 0 to 20% over 20 s. As an additional control, we unilaterally ablated all of the large RoM cells in rhombomeres 2–3, as they showed no grating responses. Fish were always able to turn in both directions after this control ablation (Fig. 5d–f). For the ventromedial cells, we unilaterally ablated 2–4 cells from each cluster, as we couldn't predict by morphology which would show the turning responses or guarantee that all cells were labeled. Nevertheless, in several cases, this resulted in a complete elimination of turning toward the ablated side (Fig. 5g–i). In cases where turning toward the ablated side was eliminated, forward swims and turns away from the ablated side were still performed normally (Supplementary Fig. 4 online). With this stochastic method, we saw, on average, a large, significant decrease in turning whenever we ablated cells in these clusters ($P < 0.001$; Fig. 5m). We observed a >90% reduction in turning toward the ablated side in 7 out of 23 ablations. Three fish had a <10% reduction and the rest had intermediate, graded phenotypes. No significant change in turning was observed when only the RoM1r cells were ablated ($P > 0.05$). We therefore argue that this small subpopulation of functionally lateralized ventromedial neurons is a necessary component of the circuit underlying turning in the optomotor response.

DISCUSSION

This study identifies groups of spinal projection neurons that are selective for visual stimuli that evoke basic swim patterns in zebrafish, and reveals, with cellular detail, the spatial organization of a vertebrate motor-control system. These functional groups are distinct and composed of an unexpectedly small number of neurons. The discrete organization that we see, which differs from previously observed distributed activity^{4,18,30}, is made apparent by the ability to evoke simple motor patterns with controlled visual stimulation. The fact that more complex behaviors are associated with distributed activation of many neurons is consistent with a model in which subsets of neurons initiate distinct components of the behavior^{31,32}.

Additional evidence for a distributed motor command has come from a number of studies that found that ablations do not abolish specific behaviors, although they can alter their latency and kinematics^{16,17,33–35}. Here, an ablation guided by an observed functional organization was able to completely abolish a specific behavior; optomotor turns in one direction were specifically eliminated by ablation of the small number of cells responsive to turn-evoking stimuli. Why do we see such a strong phenotype? Two aspects of the approach contributed to this: dynamically stabilized visual stimuli were used to elicit very specific motor patterns and responses in all of the projection neurons were assessed, thereby identifying all possible participants in the behavior.

This characterization of a functionally organized motor-control system presents new opportunities to address the development and function of systems underlying vertebrate behavior. Zebrafish are a well-established model system for vertebrate development. Hundreds of thousands of neurons and their synaptic connections are formed in the first few days of the zebrafish's life. A previous study³⁶ grouped reticulospinal neurons according to the timing of their axonal growth. Notably, there is a one to one correspondence between the classification of that study and ours; all neurons in the developmental categories 'nucMLF' and 'second wave' showed responses to forward motion, whereas all others did not. Therefore, the projection neurons active during forward slow swims constitute a distinct

developmental, as well as functional, group. Interestingly, the spinal interneurons involved in slow swimming behavior also appear a few hours later than those involved in escapes³⁷.

The spinal projection neurons link sensory processing in the brain to motor output in the spinal cord and, therefore, provide an excellent starting point for studying the sensorimotor transformations underlying behavior. Having identified which neurons control particular motor patterns, we can now ask how their activity is decoded in the spinal cord to produce the associated behavior. Substantial progress has been made recently in understanding the organization and function of specific cell types and circuits in the zebrafish spinal cord^{38–40}, encouraging the hope that a connection between descending motor commands and the resulting motor patterns is within reach. More obscure, however, is the upstream circuitry that leads to the selective activation of these descending control neurons. Recently developed optical techniques, which are capable of revealing activity and connectivity in large numbers of neurons^{41–43}, can now be focused on determining the inputs to neurons with known response selectivities and identified roles in behavior. Together, this opens up the possibility of studying complete circuits underlying complex behaviors in a vertebrate with a small, transparent brain.

METHODS

Zebrafish

We used 6–7-d-old zebrafish from AB and WIK strains in all experiments. *mitfa*^{-/-} (nacre) fish⁴⁴ were used for imaging and ablation studies, as they lack pigment in the skin, but retain normal eye pigmentation. Their behavior is indistinguishable from wild-type siblings in our assay. All experiments were approved by Harvard University's Standing Committee on the Use of Animals in Research and Training.

Behavioral setup

Zebrafish larvae swam freely in a 5-cm diameter acrylic arena. Fish were illuminated by an array of infrared light-emitting diodes and their swimming behavior was recorded at 200 Hz using an infrared-sensitive, high-speed CMOS camera (Mikrotron). Stimuli were projected directly onto a 10-cm screen 5 mm below the fish using a DLP projector (Optoma). Custom image-processing software (Visual C++, Microsoft) extracted the position and orientation of the fish at the acquisition frame rate. This information was used to update a stimulus rendered in real-time using DirectX3D (Microsoft).

Calcium imaging

Spinal projection neurons were filled as previously described¹². Briefly, a 50% (w/v) solution of dextran-conjugated calcium green (Invitrogen) was injected into the spinal cord of tricaine-anesthetized fish 24 h before imaging. Fish were embedded in 1.5% low melting-temperature agarose, paralyzed using an injection of α -bungarotoxin and imaged with a custom two-photon microscope⁴⁵, which used a pulsed Ti-sapphire laser tuned to 920 nm (Spectra Physics). The stimulus was projected from below with a DLP projector (Optoma) and passed through a red long-pass filter, which allowed simultaneous visual stimulation and fluorescence detection. In each experiment, frames were acquired at 3.6 Hz. After one or more repetitions of each stimulus, the focus was moved to a different z plane. The resulting time series were combined to yield a four-dimensional picture of the scanned volume of the brain. This image was passed through image segmentation filters in Matlab (Mathworks) to extract the volume occupied by each cell. Cell identities were assigned by hand on the basis of morphological criteria¹³. Cells with an evoked response greater than 0.1 $\Delta f/f$ to at least one stimulus direction were assigned directionality vectors and a directional preference index (DPI) calculated as in a previous study²⁷.

Two-photon laser ablation

Targeted cells were identified and a central subregion was selected from a full frame scan. The power of a mode-locked laser (850 nm) was linearly increased while the beam was scanned in a spiral pattern throughout the targeted region. Scanning was immediately terminated on the detection of brief flashes of saturating intensity, which are presumed to result from the creation of a highly localized plasma via multi-photon absorption by water molecules^{28,29}. This procedure always results in destruction of the cell despite immediately adjacent cells appearing unaffected, as verified using both a pan-neuronally expressing transgenic line (HuC:YC2.1)⁴³ and retrogradely labeled spinal projection cells.

Supplementary Material

Refer to Web version on PubMed Central for supplementary material.

Acknowledgments

The authors would like to thank M. Meister, T. Bonhoeffer, J.R. Sanes, B.P. Olveczky, M.C. Smear and J.E. Dowling for valuable comments on the manuscript, D.M. O'Malley for advice on experimental techniques, A.F. Schier for generous help with fish rearing and O.C. Orger for assistance with data analysis. This work was supported by postdoctoral fellowships from the Helen Hay Whitney Foundation (M.B.O.) and Human Frontier Science Program (J.H.B.), and US National Institutes of Health grant R01 EY014429-01A2 and funding from the McKnight and Dana Foundations (F.E.).

References

1. Orlovsky, GN.; Deliagina, TG.; Grillner, S. *Neuronal Control of Locomotion*. Oxford University Press; New York: 1999.
2. Rossignol S, Dubuc RJ, Gossard JP. Dynamic sensorimotor interactions in locomotion. *Physiol. Rev* 2006;86:89–154. [PubMed: 16371596]
3. Zelenin PV. Activity of individual reticulospinal neurons during different forms of locomotion in the lamprey. *Eur. J. Neurosci* 2005;22:2271–2282. [PubMed: 16262665]
4. Deliagina TG, Zelenin PV, Orlovsky GN. Encoding and decoding of reticulospinal commands. *Brain Res. Brain Res. Rev* 2002;40:166–177. [PubMed: 12589915]
5. Korn H, Faber DS. The Mauthner cell half a century later: a neurobiological model for decision-making? *Neuron* 2005;47:13–28. [PubMed: 15996545]
6. Gahtan E, Baier H. Of lasers, mutants and see-through brains: functional neuroanatomy in zebrafish. *J. Neurobiol* 2004;59:147–161. [PubMed: 15007833]
7. Saint-Amant L, Drapeau P. Time course of the development of motor behaviors in the zebrafish embryo. *J. Neurobiol* 1998;37:622–632. [PubMed: 9858263]
8. Budick SA, O'Malley DM. Locomotor repertoire of the larval zebrafish: swimming, turning and prey capture. *J. Exp. Biol* 2000;203:2565–2579. [PubMed: 10934000]
9. Burgess HA, Granato M. Modulation of locomotor activity in larval zebrafish during light adaptation. *J. Exp. Biol* 2007;210:2526–2539. [PubMed: 17601957]
10. Kimmel CB, Powell SL, Metcalfe WK. Brain neurons which project to the spinal cord in young larvae of the zebrafish. *J. Comp. Neurol* 1982;205:112–127. [PubMed: 7076887]
11. Lee RK, Eaton RC. Identifiable reticulospinal neurons of the adult zebrafish, *Brachydanio rerio*. *J. Comp. Neurol* 1991;304:34–52. [PubMed: 2016411]
12. O'Malley DM, Kao YH, Fetcho JR. Imaging the functional organization of zebrafish hindbrain segments during escape behaviors. *Neuron* 1996;17:1145–1155. [PubMed: 8982162]
13. Metcalfe WK, Mendelson B, Kimmel CB. Segmental homologies among reticulospinal neurons in the hindbrain of the zebrafish larva. *J. Comp. Neurol* 1986;251:147–159. [PubMed: 3782495]
14. Gahtan E, O'Malley DM. Visually guided injection of identified reticulospinal neurons in zebrafish: a survey of spinal arborization patterns. *J. Comp. Neurol* 2003;459:186–200. [PubMed: 12640669]

15. Nissanov J, Eaton RC, DiDomenico R. The motor output of the Mauthner cell, a reticulospinal command neuron. *Brain Res* 1990;517:88–98. [PubMed: 2376010]
16. Liu KS, Fetcho JR. Laser ablations reveal functional relationships of segmental hindbrain neurons in zebrafish. *Neuron* 1999;23:325–335. [PubMed: 10399938]
17. Burgess HA, Granato M. Sensorimotor gating in larval zebrafish. *J. Neurosci* 2007;27:4984–4994. [PubMed: 17475807]
18. Gahtan E, Sankrithi N, Campos JB, O'Malley DM. Evidence for a widespread brain stem escape network in larval zebrafish. *J. Neurophysiol* 2002;87:608–614. [PubMed: 11784774]
19. Briggman KL, Abarbanel HD, Kristan WB Jr. Optical imaging of neuronal populations during decision-making. *Science* 2005;307:896–901. [PubMed: 15705844]
20. Wu JY, Cohen LB, Falk CX. Neuronal activity during different behaviors in *Aplysia*: a distributed organization? *Science* 1994;263:820–823. [PubMed: 8303300]
21. Bosch TJ, Maslam S, Roberts BL. Fos-like immunohistochemical identification of neurons active during the startle response of the rainbow trout. *J. Comp Neurol* 2001;439:306–314. [PubMed: 11596056]
22. Zelenin PV, Orlovsky GN, Deliagina TG. Sensory-motor transformation by individual command neurons. *J. Neurosci* 2007;27:1024–1032. [PubMed: 17267556]
23. Wiersma CA, Ikeda K. Interneurons commanding swimmeret movements in the crayfish, *Procambarus clarkii* (Girard). *Comp. Biochem. Physiol* 1964;12:509–525. [PubMed: 14206963]
24. Pearson KG. Common principles of motor control in vertebrates and invertebrates. *Annu. Rev. Neurosci* 1993;16:265–297. [PubMed: 8460894]
25. Orger MB, Smear MC, Anstis SM, Baier H. Perception of fourier and non-fourier motion by larval zebrafish. *Nat. Neurosci* 2000;3:1128–1133. [PubMed: 11036270]
26. Borla MA, Palecek B, Budick S, O'Malley DM. Prey capture by larval zebrafish: evidence for fine axial motor control. *Brain Behav. Evol* 2002;60:207–229. [PubMed: 12457080]
27. Euler T, Detwiler PB, Denk W. Directionally selective calcium signals in dendrites of starburst amacrine cells. *Nature* 2002;418:845–852. [PubMed: 12192402]
28. Chung SH, Clark DA, Gabel CV, Mazur E, Samuel AD. The role of the AFD neuron in *C. elegans* thermotaxis analyzed using femtosecond laser ablation. *BMC Neurosci* 2006;7:30. [PubMed: 16600041]
29. Vogel A, Venugopalan V. Mechanisms of pulsed laser ablation of biological tissues. *Chem. Rev* 2003;103:577–644. [PubMed: 12580643]
30. Leonardo A, Fee MS. Ensemble coding of vocal control in birdsong. *J. Neurosci* 2005;25:652–661. [PubMed: 15659602]
31. d'Avella A, Saltiel P, Bizzi E. Combinations of muscle synergies in the construction of a natural motor behavior. *Nat. Neurosci* 2003;6:300–308. [PubMed: 12563264]
32. Bizzi E, d'Avella A, Saltiel P, Tresch M. Modular organization of spinal motor systems. *Neuroscientist* 2002;8:437–442. [PubMed: 12374428]
33. Gahtan E, O'Malley DM. Rapid lesioning of large numbers of identified vertebrate neurons: applications in zebrafish. *J. Neurosci. Methods* 2001;108:97–110. [PubMed: 11459623]
34. Zottoli SJ, Newman BC, Rieff HI, Winters DC. Decrease in occurrence of fast startle responses after selective Mauthner cell ablation in goldfish (*Carassius auratus*). *J. Comp. Physiol. [A]* 1999;184:207–218.
35. Gahtan E, Tanger P, Baier H. Visual prey capture in larval zebrafish is controlled by identified reticulospinal neurons downstream of the tectum. *J. Neurosci* 2005;25:9294–9303. [PubMed: 16207889]
36. Mendelson B. Development of reticulospinal neurons of the zebrafish. II. Early axonal outgrowth and cell body position. *J. Comp. Neurol* 1986;251:172–184. [PubMed: 3782497]
37. Kimura Y, Okamura Y, Higashijima S. alx, a zebrafish homolog of Chx10, marks ipsilateral descending excitatory interneurons that participate in the regulation of spinal locomotor circuits. *J. Neurosci* 2006;26:5684–5697. [PubMed: 16723525]
38. Bhatt DH, McLean DL, Hale ME, Fetcho JR. Grading movement strength by changes in firing intensity versus recruitment of spinal interneurons. *Neuron* 2007;53:91–102. [PubMed: 17196533]

39. McLean DL, Fan J, Higashijima S, Hale ME, Fetcho JR. A topographic map of recruitment in spinal cord. *Nature* 2007;446:71–75. [PubMed: 17330042]
40. Chong M, Drapeau P. Interaction between hindbrain and spinal networks during the development of locomotion in zebrafish. *Dev. Neurobiol* 2007;67:933–947. [PubMed: 17506502]
41. Niell CM, Smith SJ. Functional imaging reveals rapid development of visual response properties in the zebrafish tectum. *Neuron* 2005;45:941–951. [PubMed: 15797554]
42. Sato T, Hamaoka T, Aizawa H, Hosoya T, Okamoto H. Genetic single-cell mosaic analysis implicates ephrinB2 reverse signaling in projections from the posterior tectum to the hindbrain in zebrafish. *J. Neurosci* 2007;27:5271–5279. [PubMed: 17507550]
43. Higashijima S, Masino MA, Mandel G, Fetcho JR. Imaging neuronal activity during zebrafish behavior with a genetically encoded calcium indicator. *J. Neurophysiol* 2003;90:3986–3997. [PubMed: 12930818]
44. Lister JA, Robertson CP, Lepage T, Johnson SL, Raible DW. nacre encodes a zebrafish microphthalmia-related protein that regulates neural crest–derived pigment cell fate. *Development* 1999;126:3757–3767. [PubMed: 10433906]
45. Denk W, Strickler JH, Webb WW. Two-photon laser scanning fluorescence microscopy. *Science* 1990;248:73–76. [PubMed: 2321027]

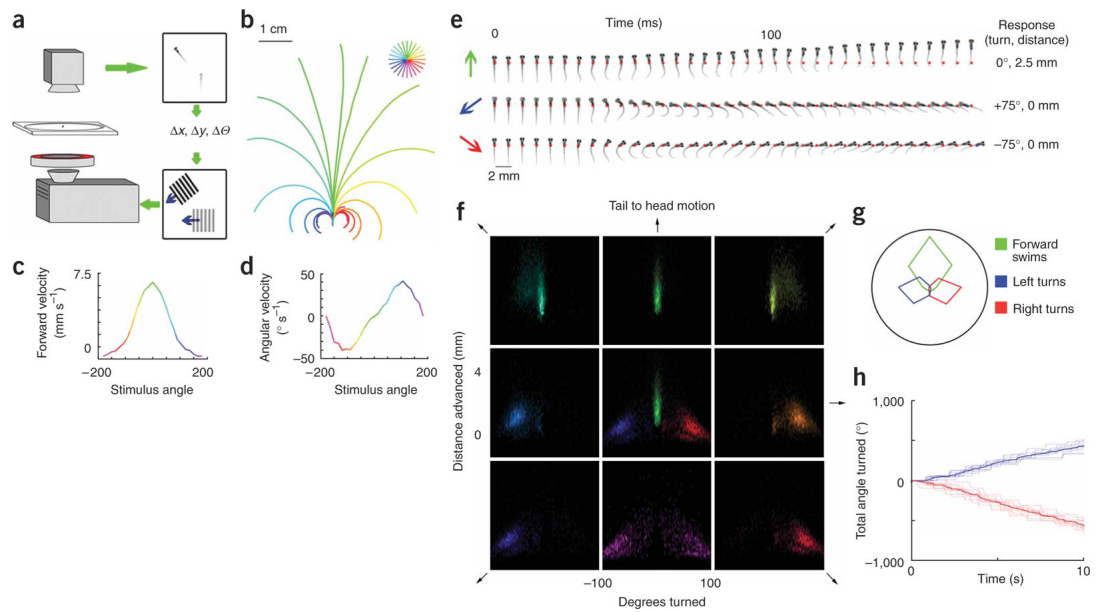


Figure 1.

Behavioral responses to drifting gratings. **(a)** Schematic of the behavioral set up. **(b)** Average trajectories of six fish responding to gratings drifting at 24 equally spaced directions relative to their body axis. Trajectories are color coded according to stimulus direction as shown in the key, with up representing forward, or tail to head, motion (green). The fish, superimposed for scale, is shown at the start position. Gratings have a spatial period of 1 cm, 5 mm below the fish, and drift with a temporal frequency of 1 Hz for 6 s. **(c,d)** Tuning of swimming parameters to grating direction for the same six fish. **(e)** High-speed kinematics of the swim bouts. Images of a fish taken at 5-ms intervals during three modes of swimming are presented from left to right. Colored arrows show the stimulus direction. Red dots indicate the starting position of the fish, the blue dot in the last frame indicates its final position and the overall trajectory is described to the right. **(f)** Distributions of swim bout parameters, forward motion and change in angle of the fishes' body axis in response to eight directions of motion (10 fish, 22,540 swim events). The fish viewed gratings of 50% contrast with the same spatiotemporal parameters as in **b**. To measure a baseline swimming distribution, we held the gratings stationary relative to the fish for 5 s and then let the gratings drift for 5 s. Each swim bout was characterized in terms of distance moved along the fishes' initial heading and the angle through which the body axis turned. Distributions are color coded by stimulus direction, with the peak of the distribution set to the maximum intensity. The eight panels representing the four cardinal and four oblique directions are arranged in a square, with tail-to-head motion at the top. The center panel shows the distributions for tail-to-head (green), back left (blue) and back right (red) stimulus motion superimposed. **(g)** Polar plot of swim-type frequency (forward swim, 0–5 mm forward, <10° turned; turns, >30°) versus stimulus direction. **(h)** Cumulative turning of one fish in response to multiple 10-s presentations of back left (+135°, blue) and back right (-135°, red) motion. Bold line indicates the mean response.

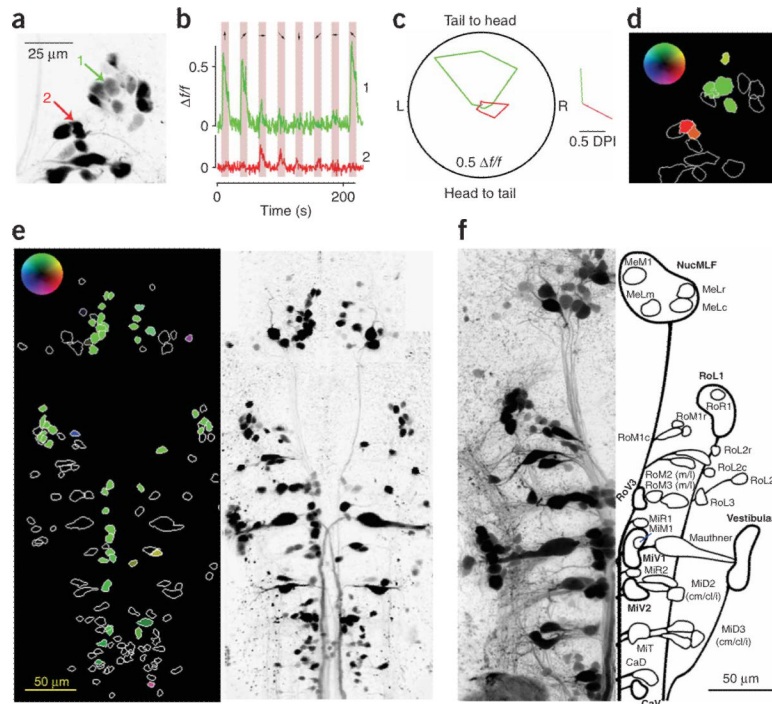


Figure 2.

Measuring calcium responses in spinal projection neurons. **(a)** Z projection of data acquired during calcium imaging at different z planes. The image is shown with inverted luminance here and in subsequent figures for visual clarity; all images are presented rostral side up. Two cells are indicated, and analysis of their calcium signals is shown to the right. **(b)** Mean fluorescence traces from the three-dimensional regions of interest that defined the two cells in **a**. The stimulus consisted of sinusoidal gratings drifting in eight different directions presented for 10 s each (shaded regions). The directions are indicated by arrows. **(c)** Polar plot showing time-averaged fluorescence changes for the eight directions of motion for the same two cells. The directionality vectors are shown to the right. **(d)** The projected outlines of all 16 cells shown in **a** are color coded according to their directionality vector using the inset look-up table (maximum intensity corresponds to 0.5 DPI). **(e)** We analyzed 151 labeled neurons in one fish as in **a–d**. **(f)** Schematic of our cell classification system; thin lines represent single neurons and bold lines denote groups based on a z projection of cells retrogradely labeled using Texas Red dextran (Invitrogen).

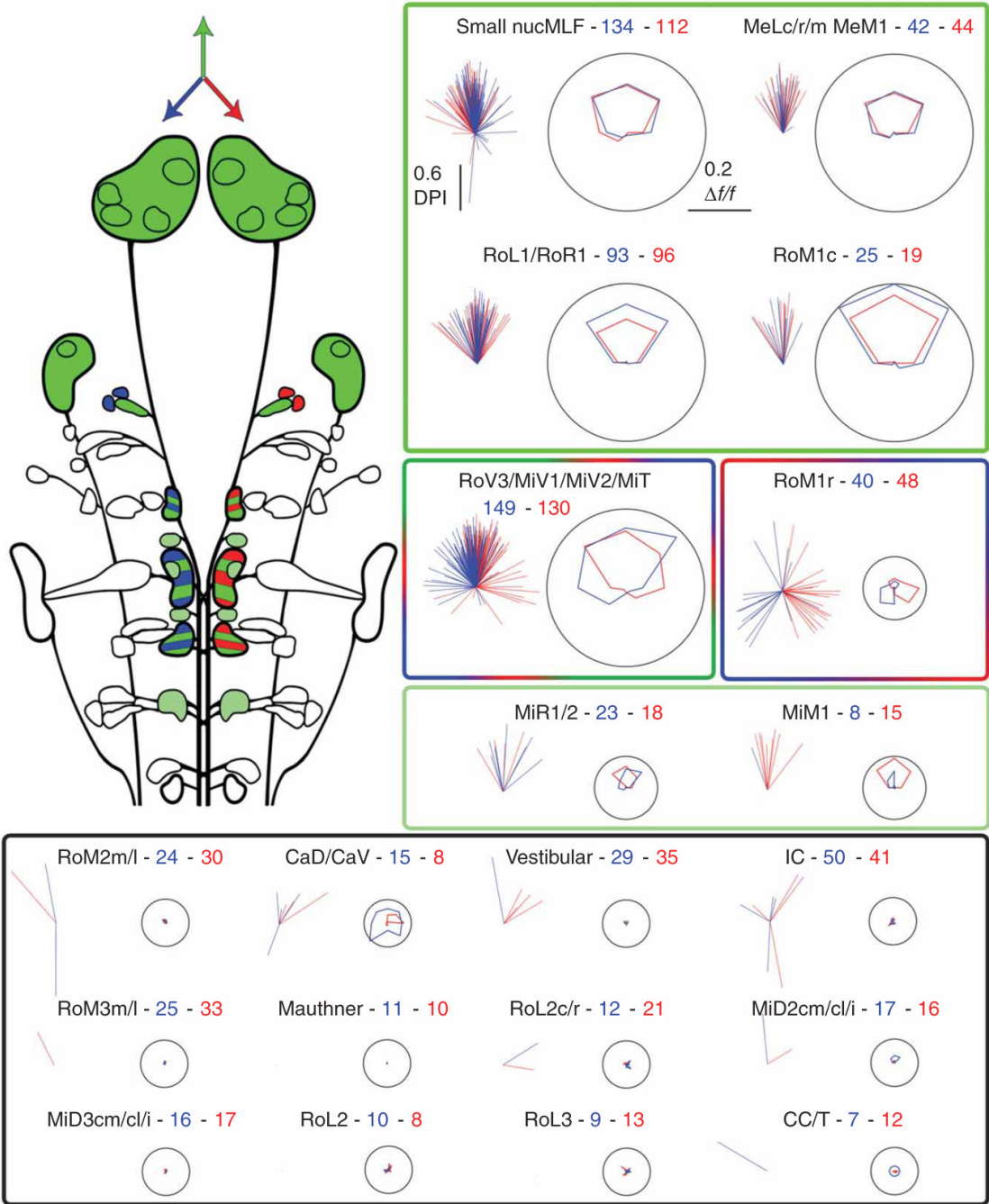


Figure 3. Summary of direction tuning of all spinal projection neurons. Top left, schematic summary of the directional preference of spinal projection neurons. Cells that preferred tail-to-head motion are colored green, cells that had a left or right preference are colored blue or red, respectively, and mixed populations are striped. Right and bottom, two plots are shown for each cell group. The left plot of each pair shows the directionality vectors for every responsive cell in a group and the right plots give the average tuning curves for the population, shown in polar form as in Figure 2c. Data from cells on the right side of the brain are shown in red, data from left cells are in blue, and up represents the tail-to-head direction. The label for each plot gives the category name followed by the number of cells

recorded on the left and the right side of the brain, respectively. The colored boxes group functionally similar classes of neurons according to their stimulus preference (forward, green; right and left turns, red and blue, respectively; no response, black).

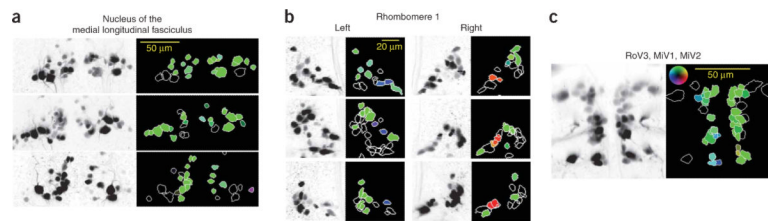


Figure 4.

Spatial distribution of visually responsive cells. Examples of the response distribution in different fish are shown here. **(a)** Bilaterally labeled nucMLF cells in three different fish with a z projection on the left and color coding by directionality vectors on the right, as presented in Figure 2. **(b)** Three examples of rhombomere 1 cell groups from left and right brain. Left and right motion preference was restricted to small rostral RoM cells and was consistent across fish. **(c)** Responses in the ventromedial portion of rhombomeres 3–5 in a fish with good bilateral labeling. Each group contains a mixture of forward and turn-stimuli preferences.

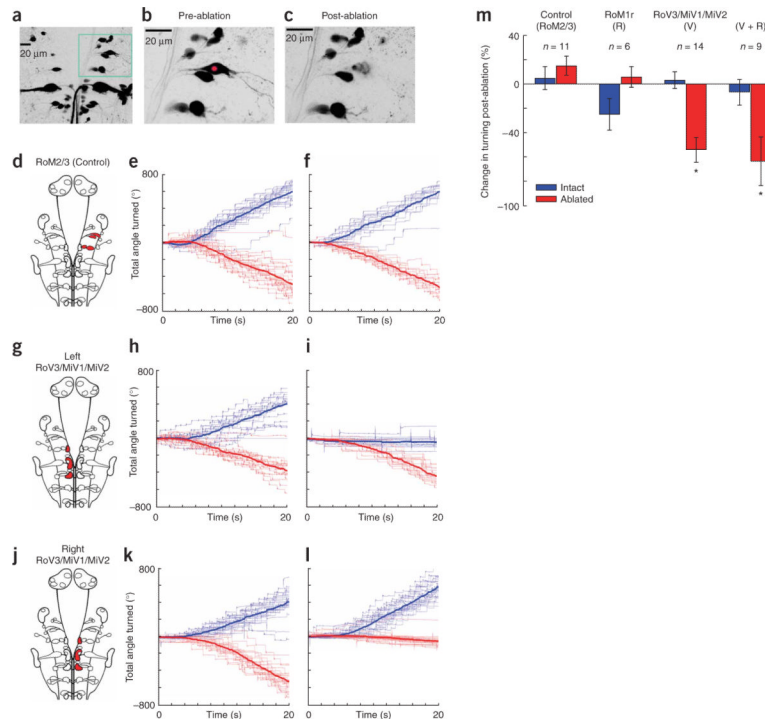


Figure 5. Laser ablation of turning-selective neurons. (a) Z projection of spinal projection neurons labeled with Texas Red dextran. (b,c) A right RoM2l neuron before and after laser ablation. The cell and its processes were destroyed and cell debris is visible. The adjacent RoM2m cell and its processes were unaffected. (d–f) Ablation of all the RoM cells unilaterally in rhombomeres 2 and 3 caused no phenotype. A schematic image indicating which neurons were selected is shown in d. The fish were tested before and after ablation using gratings drifting in two directions, back left and back right. The results of one such ablation are shown in e and f. The cumulative turning responses to many repetitions of the stimulus are plotted, with those to back left in blue, back right in red, and the mean turning is shown in bold (as in Fig. 1h). There is no obvious difference between the pre- and post-ablation behavior. (g–i) Ablation of 8–10 ventromedial cells in the left RoV3–MiV2 region can completely eliminate stimulus-evoked turns toward the ablated side. (m) Average ablation phenotypes. Change in turning following ablation is expressed as a percentage change from pre-ablation behavior (–100 indicates that the fish no longer turned and +100 indicates that the fish turned twice as much). Unilateral ablation of RoM2 and 3 cells or rostral RoM1 cells had no significant effect on turning. However, ablation of ventromedial cells unilaterally, alone or in conjunction with a RoM1r ablation, caused a severe deficit in turning with respect to control fish ($P < 0.001$; $n = 14$ and 9, two-tailed Student's t -test, error bars indicate s.e.m.).